CHEMIJA. 2019. Vol. 30. No. 2. P. 69–77

Investigation of the properties of Cr coatings deposited in an improved Cr(III) electrolyte

Gedvidas Bikulčius,

Asta Češūnienė*,

Tadas Matijošius,

Aušra Selskienė,

Vidas Pakštas

Institute of Chemistry,
CPST (Center for Physical Sciences and Technology),
3 Saulėtekio Avenue,
10222 Vilnius, Lithuania

In this study, mechanical and tribological properties of Cr coatings obtained from a Cr(III) sulfate bath with addition of the heterocyclic compound (HCC) prepared on mild steel have been investigated. The chromium plating electrolyte containing the HCC additive enables us to deposit the Cr coatings at low (20°C) temperature and low current densities. Small amounts (from 20 to 60 mgl^{-1}) of HCC were added to the Cr(III) sulfate bath in order to study the effects of HCC on coating formation. At an optimal concentration of 40 mgl^{-1}, the HCC additive to the solution ensures a high surface microhardness of the Cr deposits obtained ($HV_{0.05}$ = 1036 kg mm^{-2}) without a subsequent heat treatment. The dry sliding wear tests have shown that the Cr coatings have both a low friction coefficient and a low wear rate. The Cr(III) bath with the HCC additive is more eco-friendly and requires less energy compared with a conventional Cr(III) process.

Keywords: trivalent chromium, hardness, XRD, friction coefficient, wear rate

INTRODUCTION

According to EU Regulation (EC) No. 1907/2006 ('REACH') the use of chromium trioxide baths for functional and decorative chromium plating has been limited since 1 September 2017. Thus, Cr(III) can be used as the main source of Cr ions, because it is considered 500 to 1000 times less toxic than hexavalent chromium [1–3]. Lately ever more exacting environmental requirements are imposed upon deposition of chromium coatings [4]. $CrCl_3$ has become the most popular source of Cr(III) ions [5, 6].

Cr(III) electrolytes, in current use allowing deposition of functional Cr(III) coatings, contain various additives, most popular among them being ammonium compounds: NH_4Cl [6], $(NH_4)_2SO_4$ [7] and NH_4Br [8, 9]. Unfortunately, they are undesirable as they are difficult to remove from spent Cr(III) electrolytes.

Besides, the energy consumption aspect, which is determined by the current density (i_c) and chromium plating electrolyte temperature, is also very important. Normally, when depositing Cr coatings in the trivalent chromium plating electrolyte on iron, i_c is in the range from 30 to 50 A dm^{-2} [5, 10], and the working electrolyte temperature is in the range from 30 to 50°C [5, 10].

Therefore, it is of great importance to search for more environment-friendly and energy efficient Cr(III) electrolytes.

The aim of this work was to formulate a new chromium plating electrolyte based on Cr(III), which would be $CrCl_2$-free and ammonium compounds-free, and would operate at lower current densities (i_c) and lower chromium plating electrolyte temperatures.

* Corresponding author. Email: asta.cesuniene@ftmc.lt

EXPERIMENTAL

Preparation of specimens

Chromium coatings were electrodeposited on a mild steel (Fe-0.36 Mn, in wt.%) substrate from the electrolytes listed below in the Table. These chromium electrolytes based on the SO^{2-}_4 oxalate electrolyte were chosen because, while in use, Cl_2 gas is not released at the anode [11].

All solutions were prepared using distilled water and analytical grade chemicals (manufacturer AppliChem GmbH). The mild steel substrate was also treated mechanically polishing with silicon sandpaper up to #600 grit. After that, the samples were washed with distilled water, soaked in a hot 20 vol% HCl solution, washed again with distilled water and then immediately placed in a plating bath. The electrolyte pH was adjusted using H_2SO_4 or KOH. The bath of 1 l volume with vertical Pt (with an area of 2 × 4 cm^2) anodes and a cathode between them was maintained at constant temperature.

The cathode (substrate) and anode were disposed within the bath at a distance of 25 mm. Chromium deposits were obtained on both sides of the specimen (one side area was 1 cm^2). The cathode/anode ratio was 1:4. Chromium electroplating was performed without separation of the anodic and cathodic compartments. The deposition thickness was 6 μm.

In pursuit of high environmental standards we modified the Cr(III) sulfate–oxalate electrolyte [10], diminished the coating deposition current density from 45 to 40 A dm^{-2} and the working electrolyte temperature from 50 to 20°C (room temperature) and added heterocyclic compound 5- nitro-2- furaldehyde semicarbazone, 97% solid produced by a Sigma-Aldrich. This compound was designed as HCC additive (Table).

For comparison purposes, Cr coatings were deposited from both the modified Cr electrolyte free from the HCC additive and that containing the HCC additive.

Table. **Codes and compositions of Cr baths used for the electrodeposition of Cr (III) coatings**

Codes	Composition of Cr(III) bath:gl^{-1}	Deposition conditions
OXL	$Cr_2(SO_4)_3$ 6H_2O 150 $Na_2C_2O_4$ 35 H_3BO_3 30 Na_2SO_4 60 $Al_2(SO_4)_3$ 12H_2O 100 NaF 15	i_c = 45 A dm^{-2} t = 50°C t = 20 min non-stirring pH 1.6
OX1	$Cr_2(SO_4)_3$ 6H_2O 150 $Na_2C_2O_4$ 35 H_3BO_3 30 Na_2SO_4 60 $Al_2(SO_4)_3$ 12H_2O 100 NaF 15	i_c = 40 A dm^{-2} t = 20°C t = 20 min Magnetic stirring (350 rpm) pH 1.6
OX2	OX1 + 20 mgl^{-1} additive HCC	i_c = 40 A dm^{-2} t = 20°C t = 20 min Magnetic stirring (350 rpm) pH 1.6
OX3	OX1 + 40 mgl^{-1} additive HCC	i_c = 40 A dm^{-2} t = 20°C t = 20 min Magnetic stirring (350 rpm) pH 1.6
OX4	OX1 + 60 mgl^{-1} additive HCC	i_c = 40 A dm^{-2} t = 20°C t = 20 min Magnetic stirring (350 rpm) pH 1.6

Characterizations

A Helios NanoLab 650 DualBeam workstation (FEI) was used for chromium coatings surface (SEM). Measurements of deposit thickness were done by using the weight and cross-section methods. The samples were weighed before and after the electrodeposition. Several specimens were analysed by producing localised cross-sections by focused Ga ion beaming with a Helios NanoLab 650. Before the formation of cross-sections on the specimens a protective platinum (Pt) overcoat ~1 μm thick was deposited by electron and ion beams. Such a thick Pt overcoat layer helps avoid the Ga ion damage to the edge regions of the studied coating. Then the specimen was placed under the Ga ion beam exposure perpendicularly to the surface until the necessary depth was reached. SEM images of the cross-section were studied at 3 kV accelerating voltage and 6.3 pA current.

The measurements of deposit thickness were done by using the cross-section method.

XRD patterns of the films were measured using an X-ray diffractometer SmartLab (Rigaku) equipped with a 9 kW rotating Cu anode X-ray tube. The grazing incidence (GIXRD) method was used in a 2θ range of 15–80°. The angle between the parallel beam of X-rays and the specimen surface (angle) was adjusted to 0.5°. Phase identification was performed using the software package PDXL (Rigaku) and ICDD powder diffraction data-base PDF-4+ (2016 release).

The crystallite size was calculated using the graphical Halder–Wagner method implemented in the PDXL software package (Rigaku). The approach is based on the graphical representation of linear relationship $(\beta/\tan\theta)^2$ vs $\beta/(\tan\theta \sin\theta)$ plot (β is XRD peak physical broadening, θ is diffraction angle).

The microhardness tests were performed on the surface of the coatings using a PTM-3 (Russia) set-up at a load of 50 g. The values of HV are the average of five indentations.

Dry sliding ball-on-plate wear tests on the coated samples were carried out in the laboratory atmosphere with a relative humidity of 30–40% at room temperature. For tribological measurements a CSM Tribometer (Anton Paar, Switzerland) was used. The ball (100Cr6 steel) of 6 mm in diameter was fixed stationary. The Cr specimen was mounted on a pre-installed tribometer module, which maintained a linear reciprocal motion with an amplitude of 4 mm, speed of 2 cm/s, load of 2N. It has been known [12] that amorphous Cr coatings are not suitable for high loadings, therefore we chose 2N loadings for friction tests. For plotting the graphs, each data point of the friction coefficient was obtained by taking an arithmetical average of the modular values from the central 80% segment of the linear path. A contact profilometer Surftest SJ-210 was used to determine wear profiles of Cr coatings. As the contact needle was scanning the surfaces horizontally, it transferred the data obtained into the Image Plus software for visualization. Wear profiles were measured after friction coefficient recording, the cross-section area of wear tracks was calculated from at least 3 measurements on different wear track locations within the same specimen. Specific wear rates (mm^3/Nm) were calculated using the following equation: $K = (Sl)/(Fd)$, where S is the average cross-section area of wear track, in mm^2; l is the length of wear track, in mm; F is the load applied, in N; d is the sliding distance, in m. The most representative wear tracks were selected for the comparison between the samples in profilometry graphs.

RESULTS AND DISCUSSION

Morphology and structure analysis

The SEM micrographs and cross-sectional images from the surface of (OXL and OX1, OX2, OX3, OX4) Cr coatings are presented in Fig. 1. It can be seen that all the deposits consist of nodules. However, the nodular size depends on the temperature of chromium plating electrolyte, current density and additive concentration. A decline in the chromium plating electrolyte temperature and i_c leads to an increased nodular size (Fig. 1b). Addition of 20 mgl^{-1} of the HCC additive to the OX1 electrolyte decreases the nodular size (Fig. 1c). An increase in the concentration of the HCC additive up to 40 mgl^{-1} (Fig. 1d) leads to a decreased nodular size compared with the data presented in Fig. 1c. A further increase in the HCC additive concentration up to 60 mgl^{-1} (Fig. 1e) does not lead to any change in the nodular size compared with the data in Fig. 1d.

In all cases (Fig. 1a–e), we observed a small number of microcracks in the Cr coatings. Pores

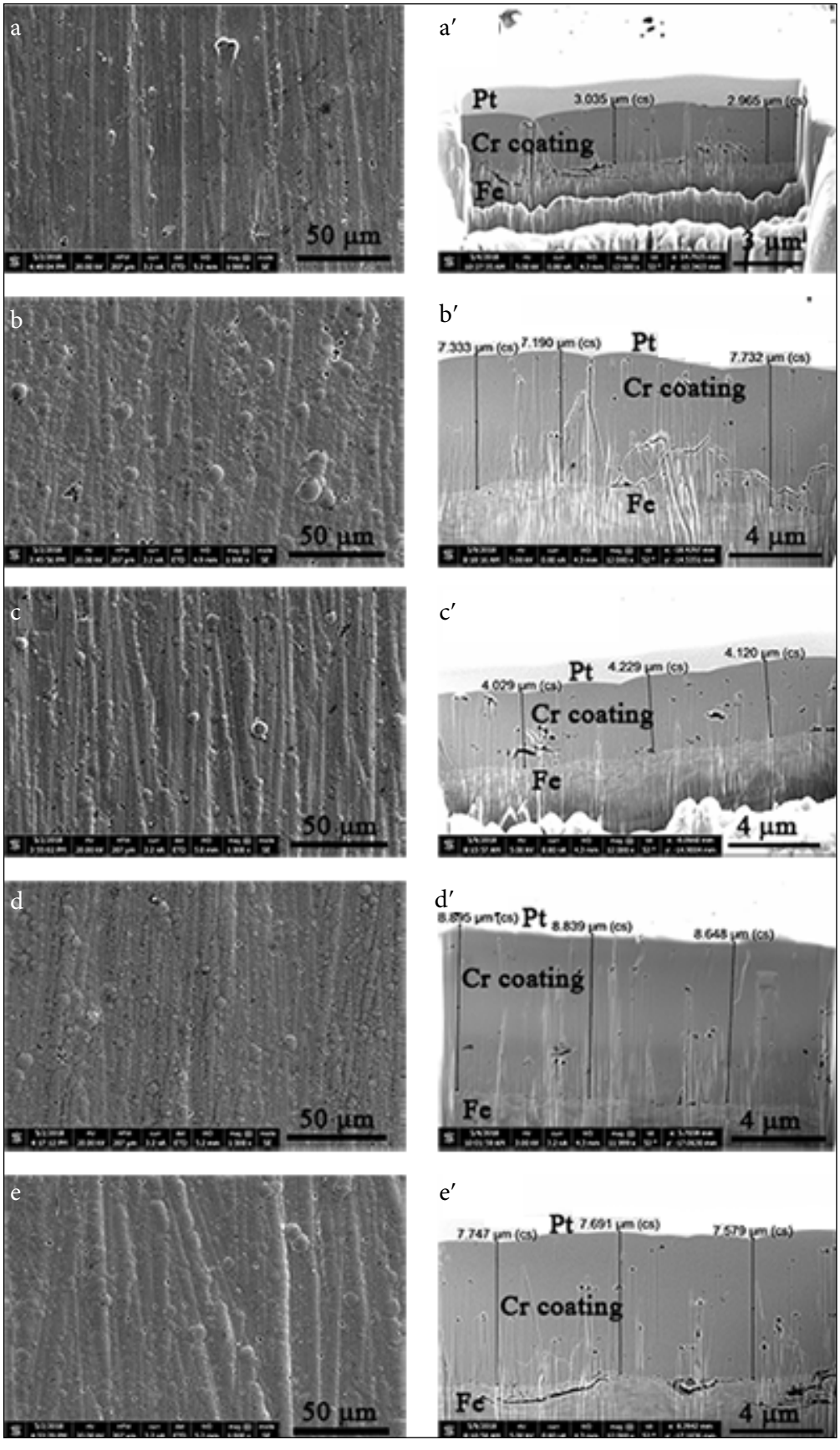

Fig. 1. SEM micrographs of the surface morphologies and the cross-sectional images for as-plated Cr coatings electrodeposited from the OXL and OX1 (HCC = 0 mgl^{-1}), OX2 (HCC = 20 mgl^{-1}), OX3 (HCC = 40 mgl^{-1}) and OX4 (HCC = 60 mgl^{-1}) electrolytes

in the form of 'exploded blisters' were also observed on all the surfaces of Cr coatings. The inner pores can also be found in the depth of Cr coatings (see cross-section in Fig. 1). It should be noted that the microcracks and pores are formed due to intensive hydrogen decomposition.

The investigation of the cross-sections of Cr coatings has shown that the thickness of the coatings obtained varied (Fig. 1a'–e'). The Cr coatings obtained from the OXL (Fig. 1a') and OX2 electrolytes had the smallest thickness (Fig. 1c'). Meanwhile the Cr coatings obtained from the OX1 (Fig. 1b)', OX3 (Fig. 1d') and OX4 (Fig. 1e') electrolytes were noticeably thicker.

The cross-sections of the Cr coatings obtained from the OXL (Fig. 1a') and OX1 electrolytes (Fig. 1b') show cracks throughout the coatings. Meanwhile the Cr coatings obtained from the OX2 (Fig. 1c'), OX3 (Fig. 1d') and OX4 electrolytes (Fig. 1e') are characterised by closed cracks, which demonstrates a direct effect of the HCC additive on the formation of Cr coatings. In all the cases dark spots can be seen, they are nothing but preserved hydrogen bubbles.

It is worth noting that a poor interface between the Fe substrate and Cr coatings is characteristic of OXL (Fig. 1a') and OX4 (Fig. 1e').

The XRD spectrum (Fig. 2) recorded for the Cr specimens has shown that the peaks located at $2\theta = 44.39$ are very broad. It can be considered that the as-deposited coatings are amorphous. On the other hand, it has been determined that the crystallite size of all the Cr coatings was quite small (about 1.0 nm). Thus, all the Cr coatings obtained may be characterised as amorphous/nanocrystallic coatings.

It is interesting how the lattice parameters of the Cr coatings vary depending on the concentration of the HCC additive. The results of lattice parameters are listed in Fig. 3. As can be seen, for

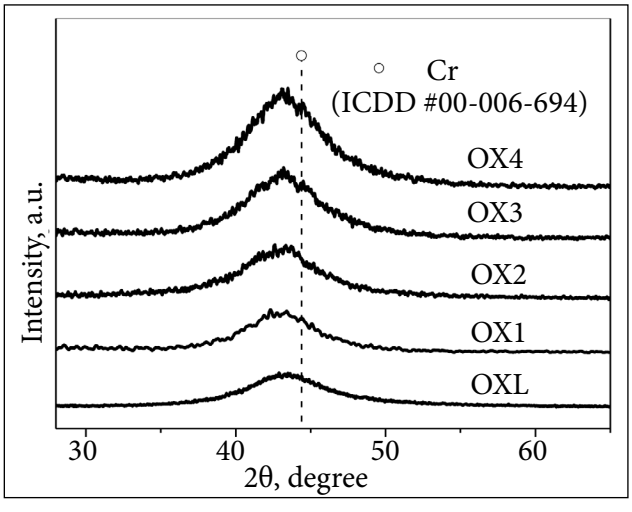

Fig. 2. XRD pattern of a mild steel substrate with the Cr coatings deposited from the OXL ($i_c = 45$ A dm^{-2}, $t = 50$°C), OX1 ($i_c = 40$ A dm^{-2}, $t = 20$°C, HCC = 0 mgl^{-1}), OX2 ($i_c = 40$ Adm^{-2}, $t = 20$°C, HCC = 20 mgl^{-1}), OX3 ($i_c = 40$ A dm^{-2}, $t = 20$°C, HCC = 40 mgl^{-1}) and OX4 ($i_c = 40$ A dm^{-2}, $t = 60$°C) baths

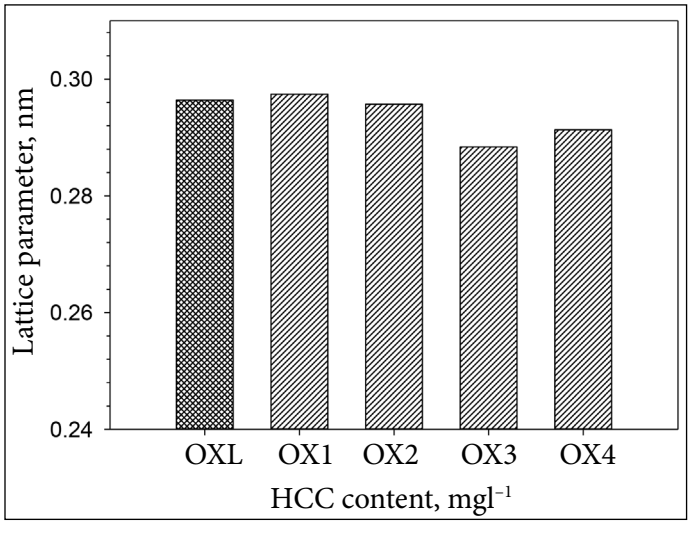

Fig. 3. Effect of the HCC concentration on the lattice parameter of Cr coatings obtained from the OXL, OX1, OX2, OX3 and OX4 electrolytes

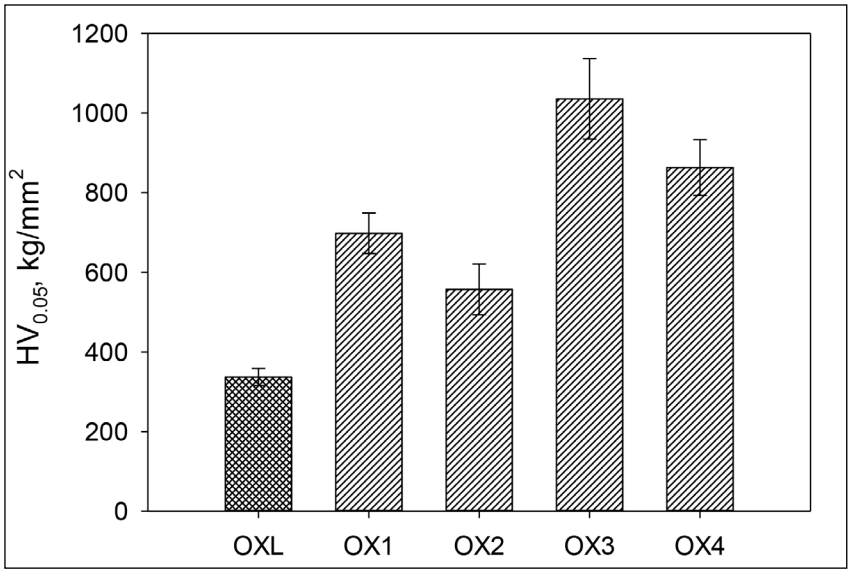

Fig. 4. Dependence of the surface microchardness (HV) of Cr coatings as a function of the deposition conditions and the concentration of HCC additive in the OXL and OX1 (0 mgl^{-1}), OX2 (20 mgl^{-1}), OX3 (40 mgl^{-1}), OX4 (60 mgl^{-1}) electrolytes. The thickness of Cr coatings is 6.0 ± 2.0 μm

the Cr coatings obtained from the OX1 electrolyte (20°C and 40 A dm^{-2} i_c) the lattice parameter value (0.2974) is the highest as compared to all other cases. Addition of the 20 mgl^{-1} HCC additive to the OX1 electrolyte lowers the lattice parameter of Cr coatings insignificantly (Fig. 3, OX2). Meanwhile, at the concentration of the HCC additive of 40 mgl^{-1} the lattice parameter of Cr coatings becomes equal to 0.2884 nm (OX3). This value of the lattice parameter is identical to that of the metallic Cr (PDF 6-694). At increased up to 60 mgl^{-1} concentrations of the HCC additive the lattice parameter also increases (Fig. 3, OX4).

Microhardness

Figure 4 illustrates the dependence of microhardness (HV) of Cr coatings on the conditions of the chromium plating process and the concentration of the HCC additive in the electrolyte. A decrease in the temperature of the Cr plating electrolyte from 50°C (Fig. 4, OXL) to 20°C (Fig. 4, OX1) and in i_c from 45 A dm^{-2} (Fig. 4, OXL) to 40 A dm^{-2} (Fig. 4, OX1) leads to a twofold increase in HV. Addition of the HCC additive to the modified Cr electrolyte makes it possible to change the value of HV. One can see that the Cr coatings obtained in the modified Cr(III) electrolyte containing

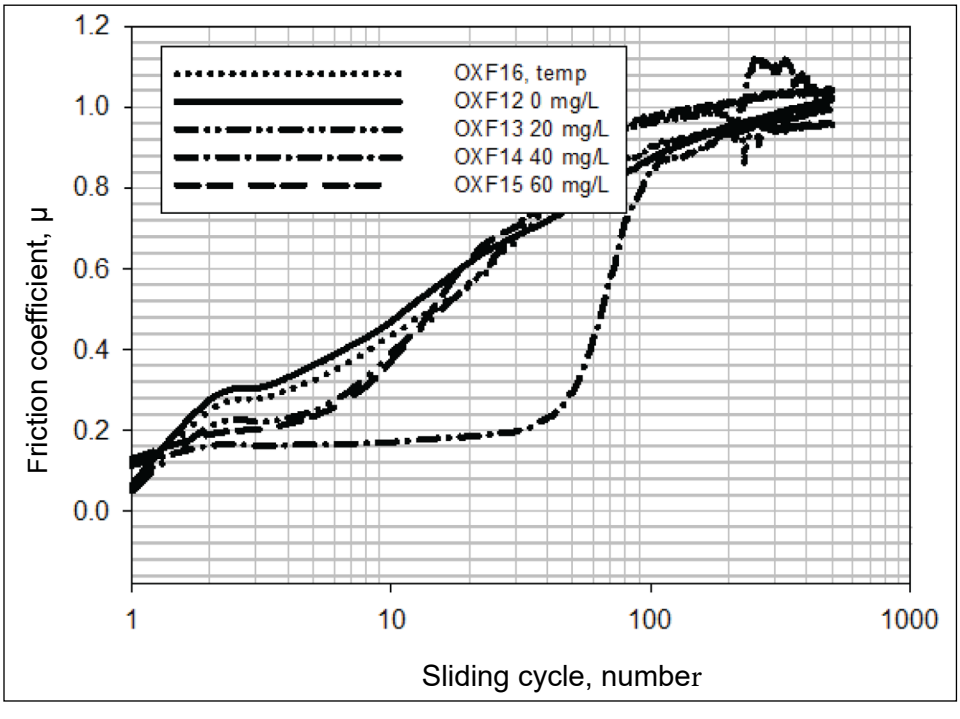

Fig. 5. The friction coefficient (μ) of Cr coatings as a function of the number of friction cycles for as-plated Cr coatings electrodeposited from OXL and OX1 (HCC = 0 mgl^{-1}), OX2 (HCC = 20 mgl^{-1}), OX3 (HCC = 40 mgl^{-1}), OX4 (HCC = 60 mgl^{-1}) electrolytes

40 mgl^{-1} of the HCC additive exhibited the highest HV value (about 1000 kg mm^{-2}) (Fig. 4, OX3). It is well to bear in mind that HV as high as this is obtained for coatings without any subsequent heat treatment. Apparently this can be explained by nodule size. In this case they are the smallest (Fig. 1d). At increased up to 60 mgl^{-1} HCC additive concentrations HV again diminishes (Fig. 3, OX4). The obtained data on the HV of chromium coatings correlate well with the lattice parameters, that is, the values of chromium coating HV increase with decreasing lattice parameters. An analogous dependence was observed when studying the Cr1-xAlxN films [13].

Analysis of friction coefficient and specific wear rate

The friction coefficients of five different Cr coatings are shown in Fig. 5. As one can see, the friction coefficients of the Cr coatings OXL and OX1 are close to each other and they both increase very rapidly from the first friction cycles. Meanwhile OX2 and OX4 are also close to each other and have lower friction coefficients as compared to those of OXL and OX1. Only the friction coefficient of OX3, i.e. with 40 mgl^{-1} of HCC additive, is low (about 0.2) and remains unchanged up to 50 cycles.

Figure 6 illustrates the dependence of the Cr coatings wear rate on the plating conditions and HCC additive concentration. As one can see, the improvement of Cr plating conditions significantly increases the specific wear rate (Fig. 6, OXL and OX1). Meanwhile, the addition of HCC additive to the Cr electrolyte allows reducing the specific wear rate of Cr coatings. The optimal HCC additive concentration (40 mgl^{-1}) makes it possible to minimise the specific wear rate of Cr coatings (Fig. 6, OX3). At increased up to 60 mgl^{-1} HCC additive concentrations the specific wear rate of Cr coatings increased again (Fig. 3, OX4). These results are in good accordance with the Archard law when the specific wear rate decreases with increasing coating microhardness [12].

Worn surface morphology

Figure 7 depicts the SEM morphologies of the worn surfaces of Cr coatings obtained from the OXL, OX1, OX2, OX3 and OX4 electrolytes. In Figs. 7a and c the cracks propagation and delamination of Cr coatings is clearly seen, consequently the wear mechanism may be characterised as adhesion/delamination. Such behaviour of the Cr coatings may also be associated with a poor interface between the Fe substrate and Cr coatings (Fig. 1a', e'). The wear mechanism of the Cr coatings obtained from the OX1 electrolyte can be characterised as adhesion (Fig. 7b). In Fig. 7c one can see a large surface deformation on the worn surface without cracks. Therefore, we can characterise the wear mechanism as plastic deformation (laminar tearing). The wear mechanism of the Cr coatings obtained from the OX3 electrolyte, i.e. at the optimal HCC concentration, proceeds according to the wear adhesive mechanism (Fig. 7d).

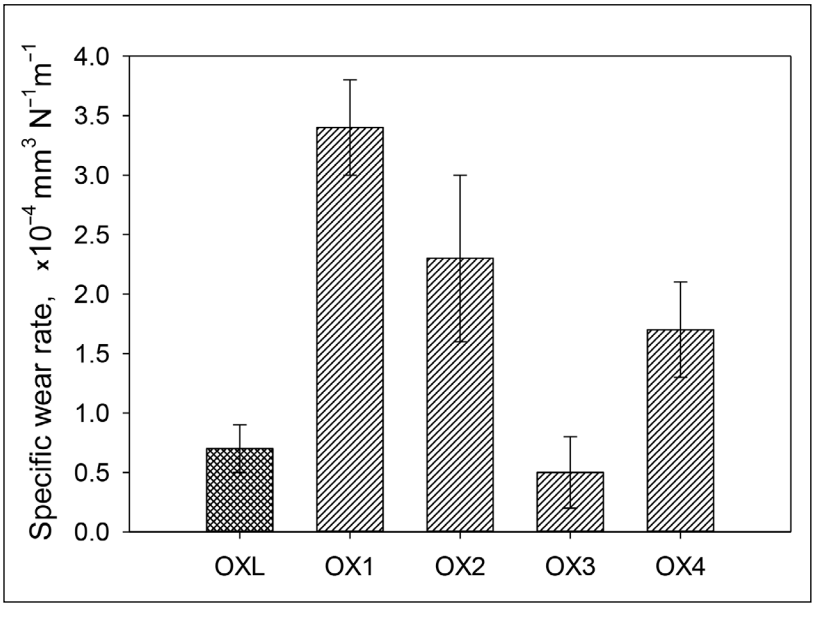

Fig. 6. Comparison of the specific wear rate of the Cr coatings electrodeposited from the OXL and OX1 (HCC = 0 mgl^{-1}), OX2 (HCC = 20 mgl^{-1}), OX3 (HCC = 40 mgl^{-1}), OX4 (HCC = 60 mgl^{-1}) electrolytes

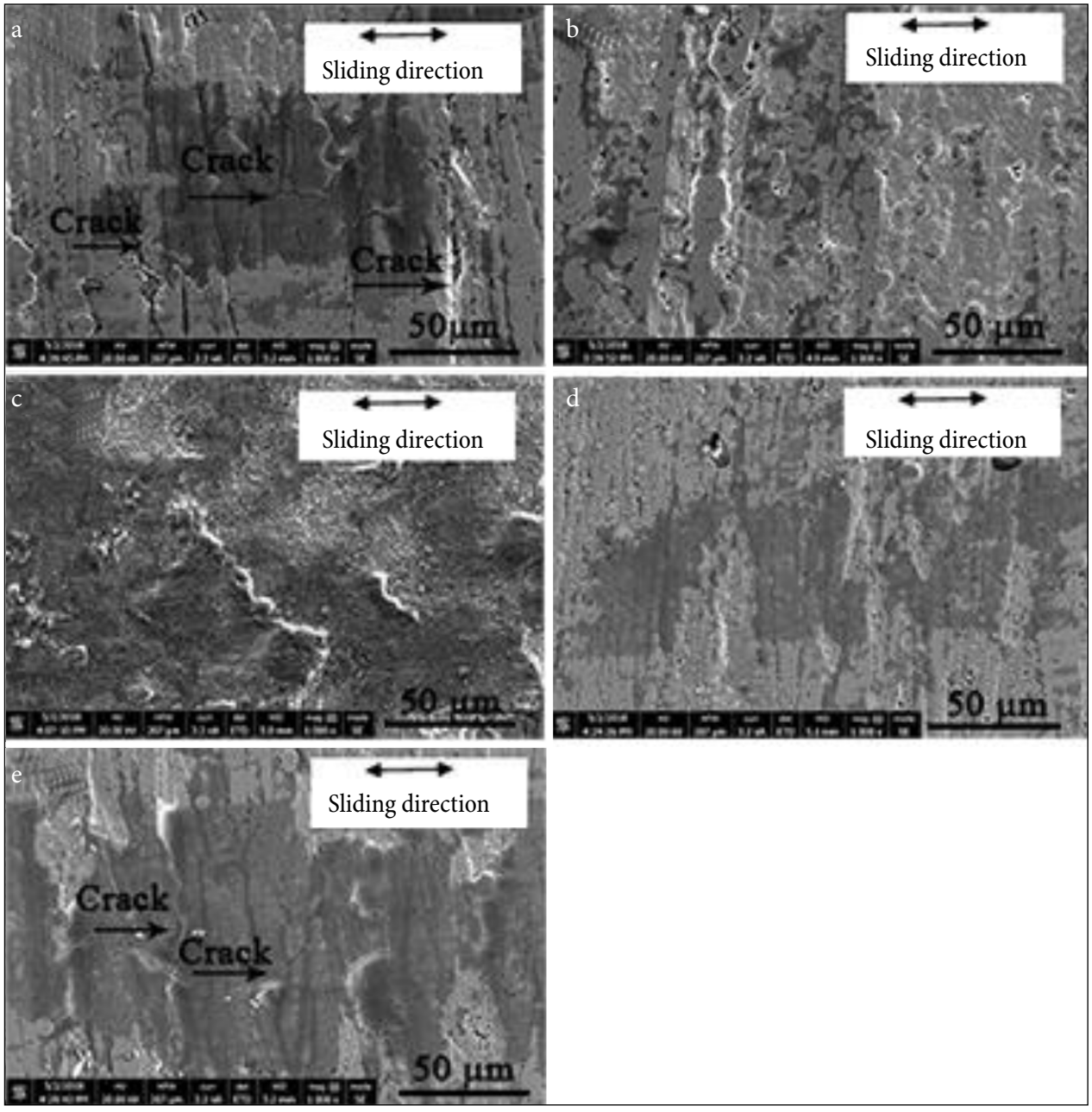

Fig. 7. SEM images of the worn surface of the Cr coatings electrodeposited from OXL and OX1 (0 mgl^{-1}), OX2 (HCC = 20 mgl^{-1}), OX3 (HCC = 40 mgl^{-1}), OX4 (HCC = 60 mgl^{-1}) electrolytes

It is obvious that there is no way to deposit high quality chromium coatings with the properties described above in an electrolyte free from the HCC additive, even all other conditions (composition of the electrolyte, temperature and current density) being the same.

CONCLUSIONS

1. The chromium plating electrolyte containing the HCC additive enables us to deposit Cr coatings at low (20°C) temperature and low current densities.

2. All the Cr coatings exhibited nodular morphology. The Cr coatings obtained from the electrolyte with the optimum concentration of 40 mgl^{-1} of the HCC additive possessed the smallest nodular size.

3. Employing the XRD method it has been determined that all the Cr coatings are amorphous/crystalline.

4. The Cr coatings obtained from the Cr electrolyte with the optimum concentration of 40 mgl^{-1} of the HCC additive exhibited the highest surface microhardness of about 1000 kg mm^{-2}.

5. The Cr coatings obtained from the Cr electrolyte with the optimum concentration of 40 mgl^{-1} of the HCC additive possessed the lowest friction coefficient of about 0.2.

6. At the HCC additive concentrations of 20, 40 and 60 mgl^{-1} in the Cr electrolyte, the wear mechanisms were as follows: plastic deformation, adhesion or adhesion/delamination, respectively.

Received 13 February 2019
Accepted 26 February 2019

References

1. L. Li, G. P. Swain, A. Howell, D. Woodbury, G. M. Swain, *J. Electrochem. Soc*., **158**, C274 (2011).
2. L. Li, K. P. Doran, G. M. Swain, *J. Electrochem. Soc.*, **160**, C396 (2013).
3. L. Li, A. L. Desouza, G. M. Swain, *J. Electrochem. Soc*., **161**, C246 (2014).
4. *Federal Register*, Vol. 77, No. 182 [https://www.gpo.gov/fdsys/pkg/FR-2012-09-19/pdf/2012-20642.pdf].
5. Ch. A. Huang, Y. W. Liu, Ch. Yu, Ch.-Ch. Yang, *Surf. Coat. Technol*., **205**, 3461 (2011).
6. A. Liang, L. Ni, Q. Liu, J. Zhang, *Surf. Coat. Technol*., **218**, 23 (2013).
7. V. Protsenko, V. Gordiienko, T. Butyrina, E. Vasileva, F. Danilov, *Turk. J. Chem*., **38**, 50 (2014).
8. S. C. Kwon, M. Kim, S. U. Park, et al., *Surf. Coat. Technol*., **183**, 151 (2004).
9. Z. Zeng, J. Zhang, *Surf. Coat. Technol*., **202**, 2725 (2008).
10. A. A. Edigaryan, V. A. Safonov, E. N. Lubnin, L. N. Vykhodtseva, G. E. Chusova, Yu. M. Polukarov, *Electrochim. Acta*, **47**, 2775 (2002).
11. V. S. Protsenko, F. I. Danilov, *Clean Techn. Environ*. Policy, **16**, 1201 (2014).
12. Z. Zeng, L. Wang, L. Chen, J. Zhang, *Surf. Coat. Technol*., **201**, 2282 (2006).
13. M. Kawate, A. Kimura, T. Suzuki, *J. Vac. Sci. Technol., A,* **20**, 569 (2002).

Gedvidas Bikulčius, Asta Češūnienė, Tadas Matijošius, Aušra Selskienė, Vidas Pakštas

CR DANGŲ, GAUTŲ PAGERINTAME CR(III) ELEKTROLITE, SAVYBIŲ TYRIMAS

S a n t r a u k a

Tirtos chromo dangų, gautų Cr(III) sulfatinėje vonioje su heterocikliniu junginiu (HCJ) ant minkšto plieno, mechaninės ir tribologinės savybės. Chromavimo elektrolitas su HCC priedu leidžia gauti Cr dangas žemoje (20 °C) temperatūroje prie žemų srovės tankių. Pastebėta, kad pridėjus į Cr(III) sulfatinę vonią mažas koncentracijas HCJ (nuo 20 mgl^{-1} iki 60 mgl^{-1}) priedo, dangų savybės kinta. Nustatyta, kad optimali HCJ (40 mgl^{-1}) koncentracija leidžia gauti kietas Cr dangas (HV0.05 = 1 036 kg mm^{-2}) jų nekaitinant. Sausos trinties bandymai parodė, kad Cr pasižymi žemu trinties koeficientu ir žema dilimo norma. Cr(III) vonia su HCJ priedu, palyginti su klasikiniu Cr(III) procesu, yra ekologiškesnė ir reikalauja mažiau energijos.